Transactions of the Materials Research Society of Japan 27 [1] 169-172 (2002)

Synthesis, Classification, and Reshaping of Gold Nanoparticles

Yuji Kawakami, Eiichi Ozawa, and Takafumi Seto*

Nano Particle Division, Vacuum Metallurgical Co., Ltd.
516 Yokota, Sanbu-machi, Sanbu-gun, Chiba 289-1297, Japan
Fax: 81-475-89-1469, e-mail: yuuji_kawakami@ulvac.com
*Research Center for Advanced Manufacturing on Nanoscale Science and Engineering,
National Institute of Advanced Industrial Science and Technology (AIST)
1-2-1 Namiki, Tsukuba, Ibaraki 305-8564, Japan
Fax: 81-298-61-7268, e-mail: t.seto@aist.go.jp

Gold nanoparticles were synthesized by Nd:YAG laser irradiation of a gold target in a low-pressure inert gas atmosphere. The ambient pressure was changed to control the particle size distribution. The distributions of the primary particle size and mobility equivalent size were measured by transmission electron microscopy (TEM) and a low-pressure differential mobility analyzer (LP-DMA), respectively. The peak of the mobility distribution shifted from several nm to tens of nm with increasing pressure and the profile changed from narrow to broad. On the other hand, the size of the primary particles was constant with pressure at several nm in diameter. From the TEM, the agglomeration of the primary particles was observed for all conditions. We tried to classify the nanoparticles using the DMA and it could have attained a very narrow size distribution of particles with the standard geometric deviation, $\sigma_g \leqq 1.1$. Furthermore, we also investigated the reshaping of the particles at high temperature to obtain individual spherical particles.

Key words: gold nanoparticles, laser ablation, size distribution, classification, reshaping

1. INTRODUCTION

Nanoparticles are now considered as one of the new materials that might provide breakthroughs in the present status of nanotechnology. The key factors that can produce these breakthroughs are their purity, size distribution, shape, crystal structure, etc. Especially, the precise control of the particle size and size distribution is very important for generating new particle characteristics depending on the size effects such as their chemical reactive characteristic, sintering characteristic and quantum effects. In particular, well-controlled gold nanoparticles have great potential due to their unique electrical and optical properties.

Many investigations on the synthesis of metal nanoparticles and their characteristics have been carried out since the 1970s. Nanoparticles have been produced by a chemical vapor synthesis [1], by a physical process such as an evaporation-condensation method [2] and laser ablation method [3-7]. The evaporation-condensation method can synthesize nanoparticles by simply evaporating the materials in an inert gaseous atmosphere using a heating device such as an induction furnace, electric arc furnace, etc. However, these methods use a crucible to hold the materials and evaporating materials often react with the crucible, which leads to their contamination. Another drawback is the difficulty in synthesizing nanoparticles of refractory materials. Therefore, only a limited number of metals can produce nanoparticles using conventional heating systems. In order to solve these problems, a CO_2 laser [3] and Nd:YAG laser [4] were used to synthesize nanoparticles, which is a very clean method due to the partial heating.

We have studied the size distribution and the evolution of metal nanoparticles produced by laser ablation for various nanoelectronic applications [5-7]. The nanoparticles produced in the generation chamber were transported to an LP-DMA [5-8] by an inert carrier gas stream. In particular, the LP-DMA was used to investigate the relationship between the synthesis conditions and the size distribution of the nanoparticles generated by the laser ablation [5-7]. The investigation of reshaping the particles at high temperature to obtain spherical nanometer-sized particles was also reported [9-11].

In this study, the classification of the nanoparticles

with diameters ≦ 50 nm using the DMA apparatus attained a very narrow size distribution of particles with a geometric standard deviation of σ_g ≦ 1.1. We also investigated reshaping the particles to obtain spherical nanoparticles by thermal annealing. As a result, we could control the shape of the nanoparticles by changing the temperature of the electric furnace, and the reshaping temperature of the nanoparticles was in good agreement with the calculated values of solid state diffusion.

2. EXPERIMENTAL

2.1 Experimental method

The apparatus (Chamber; ULVAC Materials Technology Co., Ltd., Chiba, Japan) is schematically illustrated in Fig. 1. The second harmonic (wavelength of 532 nm) of the Q-switched pulse Nd:YAG laser (Spectra-Physics, INDI-50, CA, USA) was used as the light source. The full-width at half-maximum of the pulse width was 4.5-5.5 ns. The spatial profile of the laser beam is nearly Gaussian. A round-type aperture was utilized only in the area of the high intensity laser beam. The beam was introduced into the generation chamber through a fused silica window (CVI Laser Corporation, NM, USA) and focused with a BK7 glass lens (CVI Laser Corporation, NM, USA) on the surface of the target materials. The laser fluences were 2.5 J/cm^2.

The target material was an Au disk (ϕ50 mm × t3 mm, 99.99 mass%) and it was rotated at 8 rpm during the laser irradiation. The targets were cleaned by acetone and petroleum benzine using a supersonic wave cleaner. The chamber was first evacuated to 7 × 10^{-5} Pa before the experiments. High purity helium gas (99.9999 mass%) of 1-90 kPa was then introduced into the generation chamber by controlling the flow rate of 1 *l*/min for the carrier gas and the pressure using mass flow controllers and a differential evacuation system. The nanoparticles produced in the generation chamber were carried to and then sintered/reshaped in the electric furnace, which was done prior to the LP-DMA analysis. The helium gas with flow rate of 5 *l*/min for the sheath gas was introduced into the DMA. The nanoparticles exited nozzle located in the deposition chamber and deposited on a TEM micro-grid.

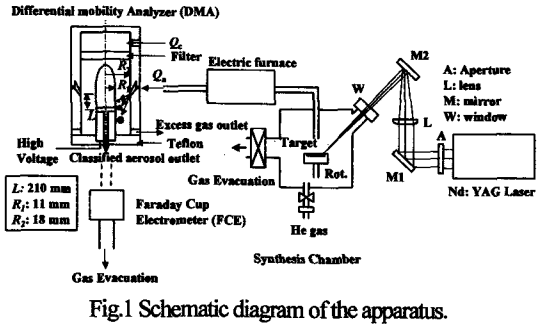

Fig.1 Schematic diagram of the apparatus.

2.2 Characterization of gold nanoparticles

The LP-DMA (a modified version of the Vienna type) [5-8] and a Faraday Cup electrometer (TSI Inc., Model 3068A, MN, USA and ADVANTEST Corporation, R8240, Tokyo, Japan) were used to measure the size distribution of the gas-borne particles. These were also used to classify the nanoparticles. The morphology of the classified nanoparticles was characterized by TEM (JEOL, Ltd., JEM-2000EX II, Tokyo, Japan).

3. RESULTS AND DISCUSSION

3.1 Synthesis and measurements of gold nanoparticles

The size distribution measurements were carried out with the LP-DMA as previously described [5-8]. Figure 2 shows the size distribution of the gold nanoparticles synthesized at pressures from 3 kPa to 90 kPa. The peak of the distribution shifted from several nm to tens of nm with increasing ambient pressure. In addition, the distribution profile changed from narrow to broad. Because the residence time of the nanoparticles in the laser-induced plasma plume and in the carrier gas flow increases with pressure, the times available for both the growth and the agglomeration of the nanoparticles increased. The same results were obtained at a higher laser fluence [12]. In order to obtain the classified particles with diameters from 30 to 50nm, we set the pressure at 20 kPa.

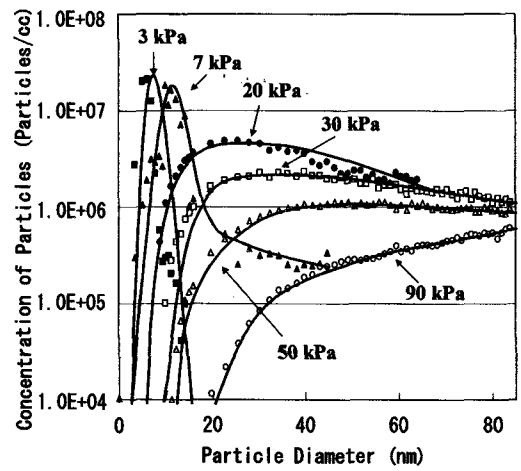

Fig.2 Comparison of size distribution of gold nanoparticles.

3.2 Classification and reshaping of gold nanoparticles

Figure 3 shows transmission electron micrographs of the classified gold nanoparticles with sizes of 30, 40, and 50 nm by the DMA for a temperature of 300 K (R. T.). The droplet-like particles at 40 and 50 nm were observed with several nm-sized particle agglomerates

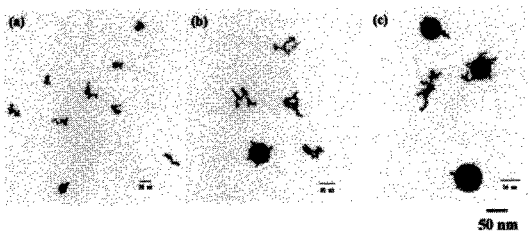

Fig.3 TEM images of classified gold nanoparticles at ambient pressure of 20 kPa.
(a) 30 nm, (b) 40 nm, (c) 50 nm.

around them. These agglomerations occurred by Brownian motion of the highly concentrated particles. We have observed the spherical tungsten nanoparticle generation at higher pressure [7] and concluded that the large sized particles of about 50 nm were produced by a kind of liquid phase splash due to the violent evaporation of the liquid or a shock wave due to the laser irradiation. From Fig. 3, it seems that the LP-DMA successfully classify the particles, however, the shape of nanoparticles was distributed. (The electrical mobility was the same, but the shape was different.) Therefore, the agglomerates were introduced into an electric furnace for reshaping by gas phase annealing.

It is well known that the gold nanoparticles completed their restructuring at a much lower temperature than those with a bulk melting point (1338 K). Thus, the mechanism leading reshaping of the primary particles is considered to be sintering due to the solid-state diffusion [13].

The sintering characteristic time was calculated from the formula proposed by Kobata et al. [14], and is as follows.

$$\tau = (2\, l_f / d_{p0})^{n}\, d_p^{m} / K = A\, d_p^{m} \exp(E / R_g T) \qquad (1)$$

where τ is the sintering time, l_f is the neck radius at the equilibrium state, d_{p0} is the primary particle diameter before heating, d_p is the primary particle diameter, K is the constant of sintering rate equation, E is the activation energy for self-diffusion, R_g is the gas constant, T is the temperature, m and n are the constants of the sintering rate equation which depend on the physical properties and dominant mass transport mechanism for sintering (m = 4, n = 6 for grain boundary diffusion or surface diffusion), and A is a constant expressed as, e.g., grain boundary diffusion [15].

$$A = \kappa T (2\, l_f / d_{p0})^{6} / 12\, b\, D_{B0}\, \gamma\, \Omega \qquad (2)$$

$$b\, D_{B0} = 3 \times 10^{-16} \exp(-110\ \mathrm{kJ} / R_g T) \qquad (3)$$

where κ, D_{B0}, b, γ, and Ω are the Boltzmann constant, the pre-exponential factor for the diffusion constant, the grain boundary width, the surface tension, and the atomic volume, respectively.

$$\tau = 6.89 \times 10^{19}\, d_p^{4}\, T \exp(110\ \mathrm{kJ \cdot mol^{-1}} / R_g T) \qquad (4)$$

where $(l_f / d_{p0}) = 0.83$, $\gamma = 1.4\ \mathrm{Nm^{-2}}$, $\Omega = 1.3036 \times 10^{-29}\ \mathrm{m^3}$, and $E = 110$ kJ/mol.

Figure 4 shows the calculated values of τ as a function of temperature and primary particle diameter using Eq. (4). The calculated time was the time needed to attain the diameter of a single particle obtained from the unification of two particles for each temperature. If the as-grown agglomerates with a 50 nm diameter pass through the heating area for 0.3 sec, the temperature needed for unification of the two particles is about 1050 K. Therefore, we fixed the sintering temperature at 1273 K for the completion of the sintering of particles with a larger than 50 nm diameter. We then classified the reshaped nanoparticles using the DMA.

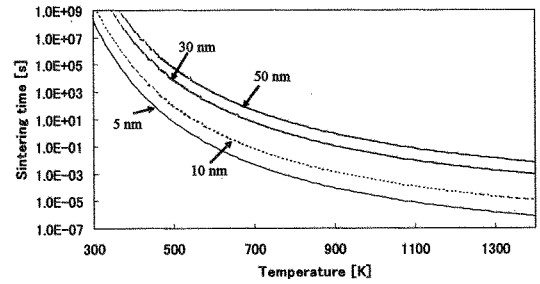

Fig.4 Relationship between sintering time and temperature of each primary particle diameter using Eq. (4).

In order to examine the effect of the heating, we tried to classify the nanoparticles that were reshaped at different temperatures. Figure 5 shows the transmission electron micrographs of the classified gold nanoparticles at a 10 nm size by the DMA with varying temperature of the electric furnace from 300 K (R. T.) to 1200 K. At 300 K, the classified particles were agglomerated by several nm-sized particles,

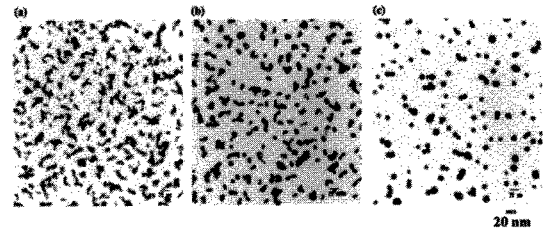

Fig.5 TEM images of 10 nm classified-nanoparticles reshaped at different temperature and ambient pressure of 3 kPa.
(a) 300 K (R. T.), (b) 600 K, (c) 1200 K.

which were also agglomerated on the TEM micro-grid. We observed spherical and elliptical particles at 600 K. These particles are still polycrystalline. Sintering definitely occurs at this temperature. Since the residence time of the nanoparticles passing through the heating area was 5×10^{-2} sec under our experimental conditions, the value of the sintering characteristic time in Fig. 4 reasonably predicts this phenomenon. The particles were completely sintered at 1200 K, because all particles were restructured to a spherical shape and were single crystalline.

Figure 6 shows transmission electron micrographs and the size distribution of the classified gold nanoparticles with a 50 nm size using the DMA at a temperature of 1273 K. We can see the faceted crystals of the nanoparticles. The first peak is close to the setting value of the DMA from Fig. 6b. The second small peak at about 70 nm is considered to be that of the doubly charged particles. However, we could still attain a very narrow size distribution of particles with a $\sigma_g \leqq 1.1$ geometric standard deviation.

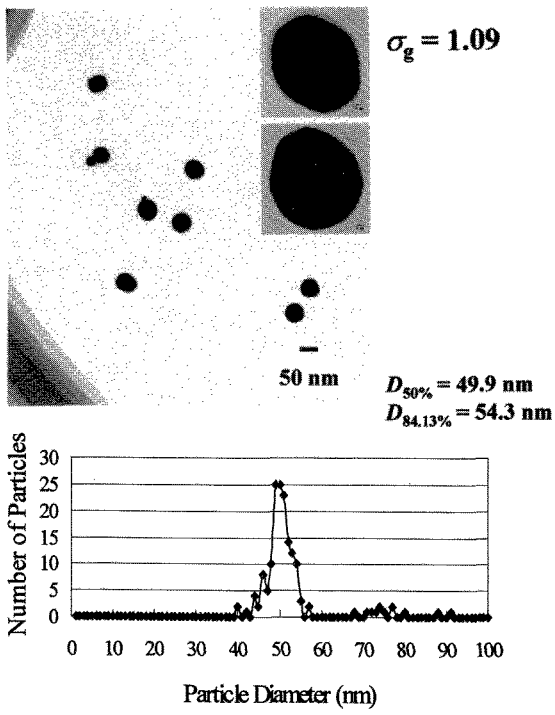

Fig.6 TEM images of 50 nm classified-nanoparticles reshaped at 1273 K and ambient pressure of 20 kPa.

4. CONCLUSION

In conclusion, gold nanoparticles were synthesized by nanosecond pulsed Nd:YAG laser ablation on a gold substrate in a low-pressure inert gas atmosphere. The ambient pressure was changed to control the particle size distribution.

The heat-treatment of the as-grown nanoparticles at a suitable temperature to accelerate the sintering of the agglomerates was done so that we obtained single crystalline nanoparticles. We could also attain a very narrow size distribution of particles with a $\sigma_g \leqq 1.1$ geometric standard deviation using our LP-DMA classification apparatus. By using this technique, we will be able to make truly artificial composites made of nm sized structures, nm sized structure films, etc., which are expected to show new characteristics for magnetic materials, memory materials, electric materials and so on. In addition, we need to further investigate the electrical and optical properties vs. size dependency of these particles.

5. ACKNOWLEDGEMENTS

We gratefully acknowledge the support of this research by the R&D Institute for Photonics Engineering (RIPE) entrusted from the Advanced Photon Processing and Measurement Technologies Program of the New Energy and Industrial Technology Development Organization (NEDO) of Japan.

6. REFERENCES

[1] A. Kato, *Ceramics Japan*, **13**, 625-33 (1978).
[2] S. Yatsuya, R. Uyeda, *Oyo Buturi*, **42**, 1067-85 (1973).
[3] M. Kato, *Jpn. J. Appl. Phys.*, **15**, 757-60 (1976).
[4] A. Matsunawa, S. Katayama, T. Ariyasu, Y. Arata, *J. High Temp. Soc.*, **13**, 30-41 (1987).
[5] Y. Kawakami, T. Seto, and E. Ozawa, *Appl. Phys. A*, **69**, S249-52 (1999).
[6] Y. Kawakami, T. Seto, Y. Yamauchi, and E. Ozawa, *Rev. Laser Eng.*, **28**, 365-69 (2000).
[7] E. Ozawa, Y. Kawakami, and T. Seto, *Scripta Materialia*, **44**, 2279-83 (2001).
[8] T. Seto, T. Nakamoto, K. Okuyama, M. Adachi, Y. Kuga, and K. Takeuchi, *J. Aerosol Sci.*, **28**, 193-206 (1997).
[9] M.H. Magnusson, K. Deppert, J.-O. Malm, J.-O. Bovin, and L. Samuelson, *J. Nanoparticle Research*, **1**, 243-51 (1999).
[10] M. Shimada, T. Seto, and K. Okuyama, *J. Chem. Eng. Jpn.*, **27**, 795-802 (1994).
[11] T. Seto, M. Shimada, and K. Okuyama, *Aerosol Sci. Tech.*, **23**, 183-200 (1995).
[12] Y. Kawakami, T. Seto, and E. Ozawa, *Appl. Surf. Sci*, (submitted).
[13] M. F. Ashby, *Acta Metallurgica*, **22**, 275-89 (1974).
[14] A. Kobata, K. Kusakabe, and S. Morooka, *AIChE J.*, **37**, 347-58 (1991).
[15] W. S. Coblentz, J. M. Dynys, R. M. Cannon, and R. L. Coble, *Mater. Sci. Res.*, **13**, 141-57 (1980).

(Received December 28, 2001; Accepted January 16, 2002)